

Topology Optimization of a Flywheel Energy Storage Rotor using a Genetic Algorithm

Thomas Hinterdorfer, Alexander Schulz, Harald Sima, Stefan Hartl and Johann Wassermann

Vienna University of Technology, Institute of Mechanics and Mechatronics,
Wiedner Hauptstraße 8-10, A-1040 Vienna, Austria,
{givenname.surname}@tuwien.ac.at

Abstract—This paper deals with topology optimization of the rotor of a flywheel energy storage system (FESS). For isotropic materials the constant stress disc (CSD) is the best choice to maximize energy density. Modern FESS are manufactured of fiber reinforced plastics (FRP), due to their high specific strength. Because of the transverse isotropic material description the optimal rotor topology changes. A genetic algorithm (GA) for nonlinear integer problems will be used to find the best rotor structure which can be manufactured within one filament winding process.

I. INTRODUCTION

Flywheel energy storage systems represent an ecologically and economically sustainable technology for decentralized energy storage. Compared to other storage technologies such as e.g. accumulators, they offer longer life cycles without performance degradation over time and usage and need almost no systematic maintenance. To achieve a high energy density FESS rotors are usually manufactured of FRP, which enables high tip speeds. For stable operation and minimal friction loss high-end FESS are supported by magnetic bearings. To minimize drag the rotor operates in a vacuum chamber. An overview and the requirements on the individual components of a FESS are given in [1].

The aim of rotor design is to maximize the energy density κ which is defined as the kinetic energy per unit mass

$$\kappa = \frac{\frac{1}{2} I_z \Omega_{max}^2}{m} \quad (1)$$

with the moment of inertia I_z , the maximum angular velocity Ω_{max} and the rotor mass m . The maximum possible energy density for an isotropic material is equal to the materials specific strength







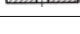
$$\kappa_{max} = \frac{X}{\rho} \quad (2)$$

where X denotes the ultimate strength and ρ the density. Moreover the reached energy density depends on the geometry. The geometry factor is defined as

$$K = \frac{\kappa}{\kappa_{max}} \quad (3)$$

and is a measure for the cost-effectiveness of the rotor shape, because a higher value of K leads to a higher amount of stored energy at constant mass. The values of K for different rotor geometries are listed in Table I, where a poisson's ratio of $\nu = 0.3$ was assumed.

Table I
GEOMETRY FACTOR K FOR DIFFERENT ROTOR CROSS-SECTIONS FOR ISOTROPIC MATERIAL WITH $\nu = 0.3$ (CF. [2])

Flywheel geometry	cross section	K
theoretical constant stress disc		1.000
real constant stress disc		0.7-0.98
conical disc		0.7-0.95
constant thickness disc		0.606
thin hollow cylinder		0.5
disc with rim		0.4-0.5
pierced constant thickness disc		0.303

When an isotropic material is assumed, the shape factor K equals one when the equivalent stress reaches its maximum value in every point of the structure with respect to some stress criterion, which corresponds to the constant stress disc. Due to the tri-axial stress state the contour of the CSD cannot be derived analytically. Some suggestions are given in [3], where an analytical function for the CSD is described. In the range of $r \leq \beta_r R_o$ the contour is given as a function of the normalized radius $\chi = r/R_o$

$$H_u(r) = h_c \left\{ e^{-\frac{B\chi^2}{2}} + \bar{\alpha} e^{-\frac{B\beta_r^2}{2}} \left[\frac{1}{2} + \frac{1}{\pi} \operatorname{atan} \left(\frac{\bar{\chi}}{a_r} \right) \right] \right\} \quad (4)$$

for $r > \beta_r R_o$ and $h < h_{max}$

$$H_u(r) = h_c e^{-\frac{B\beta_r^2}{2}} \left[\frac{1 + \alpha_r}{2} + \left(\frac{\bar{\alpha}}{\pi a_r} - B\beta_r \right) \bar{\chi} \right] \quad (5)$$

and in the case of $r > \beta_r R_o$ and $h \geq h_{max}$

$$H_u(r) = h_{max} = \alpha_r h_c e^{-\frac{B\beta_r^2}{2}} \quad (6)$$

with the radius

$$\beta_r = \left\{ \frac{2}{B\alpha_r} \left[\bar{\alpha} + \sqrt{\alpha_r^2 B(B-2+2\nu) + \bar{\alpha}^2} \right] - \frac{1+\nu}{1-\nu} \right\}^{\frac{1}{2}} \quad (7)$$

and the abbreviations $\bar{\alpha} = \alpha_r - 1$ and $\bar{\chi} = \chi - \beta_r$ and the constants B , α_r , h_c and a_r . The described function will be used as reference solution in chapter IV-A.

As a result of (2) carbon and glass fiber reinforced plastics (CFRP, GFRP) are the material of choice for high performance FESS, because of their high strength and low density. Fig. 1

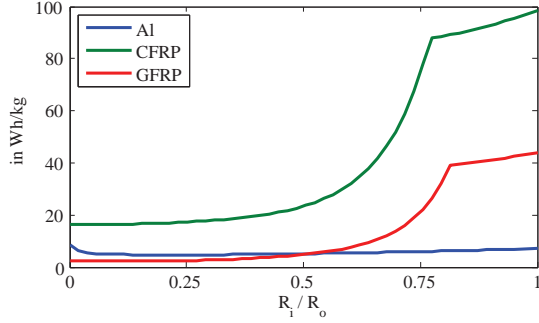


Figure 1. Energy density of a disc as function of ratio inner to outer radius for different materials

presents the energy density of a disc as a function of ratio inner radius R_i to outer radius R_o for different materials and demonstrates the potential of those materials in comparison to aluminium. The calculation was done by using the material described in chapter III-A. The maximum energy density is reached when R_i/R_o is close to 1. Then the radial stress is almost zero and the fibers are fully loaded in circumferential direction. Vice versa, at smaller values the radial stress is rather high and therefore the load is transverse to fiber direction.

Due to easy manufacturing mostly a simple cylinder is used like in [4], where the rotor is assembled of rings with different materials. It concludes that stiffer materials at increased radius leads to a decrease of radial stresses due to the different radial expansion. In [5] also a rectangular rotor shape is used which consists of several rings press-fitted into each other. This results in compressive residual stresses and therefore an increase of energy density. A low cost flywheel for rural energy storage is described in [6]. A kind of constant stress disc is used as rotor shape, which is legitim due to the quasi-isotropic rotor made of short fiber composites which is molded and than milled.

Usually for topology optimization the SIMP-method is used, which is a challenge when inertia loads are applied (cf. [7]). In [8] a turbine disk profile is optimized by metamorphic development. For this purpose the strain energy density is evaluated at the rotor surface, which decides if the structure will grow or degrade in a special position. Here only isotropic materials are considered and the objective function is not useful for flywheel applications. [9] uses an injection island genetic algorithm to optimize the rotor topology and different algorithms are compared to each other. Both papers only consider isotropic materials.

There are some subtle constructions in literature. A thick hollow cylinder is used as inertia in e.g. [10]. This cylinder is supported by a hub which is connected to the shaft. The focus lies on the hub design which is formed to enable an operation between first and second bending frequency.

II. ASSUMPTIONS AND OVERVIEW

Material transitions are always a soft spot. So this work will build up a rotor structure that is made of a single material which can be manufactured within one filament winding process. The shaft is planned to be shrink-fitted into the

Table II
MATERIAL PROPERTIES OF CFRP AND ALUMINIUM

		CFRP	Al
E_φ	longitudinal young's modulus, GPa	145.38	70
E_r	transverse young's modulus, GPa	9	70
$G_{\varphi r}$	shear modulus in φr -plane, GPa	4.97	26.9
$\nu_{\varphi r}$	poisson's ratio φr	0.24	0.3
ν_{zr}	poisson's ratio zr	0.27	0.3
ρ	density, kg/m ³	1535.5	2700
X	longitudinal tensile strength, MPa	2179	275
X'	longitudinal compressive strength, MPa	1702	275
Y	transverse tensile strength, MPa	98	275
Y'	transverse compressive strength, MPa	210	275
S	shear strength, MPa	115	275

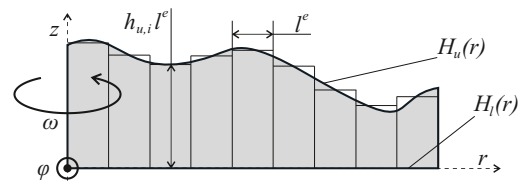


Figure 2. Discretization of the rotor geometry and parameter definitions

composite rotor. This leads to compressive residual stresses in radial direction. For the sake of simplicity the shaft will be neglected in the following optimization, which is a conservative assumption in strength analysis. Also eigenfrequencies and eigenmodes will not be considered. All calculations were done with a safety margin of 2.

In chapter III the finite element model and the used GA are described. The optimization results for isotropic as well as transverse isotropic materials are presented in chapter IV. Chapter V concludes the paper.

III. OPTIMIZATION PROBLEM

A. Finite Element Model

The properties of the applied aluminium and unidirectional CFRP with fibers oriented in circumferential direction are summarized in Table II. Together with (8) the elasticity tensor can be set up

$$G_{rz} = \frac{E_r}{2(1 + \nu_{rz})}, \quad \frac{\nu_{r\varphi}}{E_r} = \frac{\nu_{\varphi r}}{E_\varphi}, \quad E_z = E_r, \quad (8)$$

$$G_{\varphi z} = G_{\varphi r}, \quad \nu_{\varphi r} = \nu_{\varphi z}, \quad \nu_{r\varphi} = \nu_{z\varphi}, \quad \nu_{rz} = \nu_{zr}.$$

For aluminium the von Mises yield criterion and for the CFRP the Puck criterion is used ([11], [12] and [13]).

The stress calculation was performed with an axisymmetric finite element model. Quadrilateral elements with a square cross section of length l^e and linear shape functions were applied. The discretization method can be seen in Fig. 2. The z -axis is the axis of rotation and the rotor is assumed to be symmetrical with respect to the $r\varphi$ -plane. The rotor contour consists of the upper $H_u(r)$ and the lower contour $H_l(r)$. The

optimization was carried out by the use of the rate of change of the contour as optimization variable

$$H_u(r) = H_{u,0} + \int_0^r \frac{dH_u(\eta)}{d\eta} d\eta \quad (9)$$

$$H_l(r) = \int_0^r \frac{dH_l(\eta)}{d\eta} d\eta$$

where η is an integration variable. Thereby, bounds can be applied on the optimization variables to avoid large steps. The rotor is discretized with N elements along the radial direction and also the height can only change in steps of l^e , which leads to the approximation of the contour

$$H_u \left(i \leq \frac{r - R_i}{l^e} < i+1 \right) \approx \left[h_{u,0} + \sum_{i=1}^{N-1} \underbrace{(h_{u,i} - h_{u,i-1})}_{\Delta h_{u,i}} \right] l^e$$

$$H_l \left(i \leq \frac{r - R_i}{l^e} < i+1 \right) \approx \left[\sum_{i=1}^{N-1} \underbrace{(h_{l,i} - h_{l,i-1})}_{\Delta h_{l,i}} \right] l^e \quad (10)$$

where $h_{u,0}$, $\Delta h_{u,i}$ and $\Delta h_{l,i}$ are integer values. $h_{l,0}$ is zero to keep the geometry in the origin.

The vertical displacement of the nodes along the r -axis was set to zero to ensure a symmetric rotor. Also the horizontal displacement along the z -axis was set to zero. The applied inertial load is the volume force due to the angular velocity

$$F_{\text{Vol}} = \int_m r \omega^2 dm \quad (11)$$

where ω is an arbitrary angular velocity.

The stresses were evaluated in the nodes and afterwards averaged over the whole element to smooth the results and avoid numerical singularities. To evaluate the stress criterion a stress ratio R where introduced

$$\sigma_{ij}^* = \frac{\sigma_{ij}}{R} \quad (12)$$

where σ_{ij}^* denotes the stress on the failure surface of the appropriate criterion and σ_{ij} the actual stress state. The stress state is within the failure surface if $0 \leq R < 1$ is fulfilled. Higher values of R means failure. Due to linear analysis the angular velocity, which leads to failure of the structure with a safety margin S can be derived as

$$\Omega_{max} = \omega \sqrt{\frac{1}{S \cdot \max \{R(\omega)\}}} \quad (13)$$

Together with (1) the maximum energy density of a given structure can be calculated.

B. Optimization Algorithm

Due to the finite element discretization the optimization variables are integer values. This leads to the disadvantage that calculating an optimization step with a gradient based method is not possible. Therefore a genetic algorithm which

can handle integer variables is used. The fitness function is to maximize the energy density

$$\min_{\mathbf{x}} \{-\kappa\} \quad (14)$$

where \mathbf{x} is the vector of optimization variables presented later. In the following the function `ga(...)` of MATLAB R2010b with some adaptations will be used.

As a start a set of unique individuals of the optimization variables $h_{u,0}$, $\Delta h_{u,i}$, $\Delta h_{l,i}$ in (10) is generated by a creation function and the energy density is evaluated. A number of elite individuals are guaranteed to survive into the next generation. A selection function chooses parents which are then combined by a crossover function to childrens for the next generation. Afterwards the set of individuals for the following generation is filled with randomly created individuals by a mutation function. This procedure is done till the algorithm stops, which is the case if no improvement is reached within a chosen number of generations.

The creation function and mutation function are identical and are creating a random unique population, which fulfills the bounds and constraints and do not lead to intersections of the geometry. Thus it is not necessary to solve a constraint optimization problem. The crossover function randomly composes two parent genes. The parent individuals are chosen by a stochastic universal sampling as a selection function.

In the following examples the population size was 400 and ten elite individuals were used. Any other options were left default.

IV. OPTIMIZATION RESULTS

A. Isotropic Material - Constant Stress Disc

To validate the functionality of the algorithm in a first step the CSD will be calculated. For this purpose the lower contour and the inner radius were set to zero

$$H_l(r) = 0, \quad R_i = 0 \quad (15)$$

and the upper contour is optimized. The goal is a fully stressed structure. The vector of optimization variables is then

$$\mathbf{x} = \left(h_{u,0}, \Delta h_{u,1}, \dots, \Delta h_{u,N-1} \right)^T \quad (16)$$

with the length N which was chosen to be 100. The optimization bounds were defined as

$$-2 \leq \Delta h_{u,i} \leq 2 \quad (17)$$

so the maximum vertical variation was allowed to be 2 elements within one radial element step. To avoid intersections with the r -axis the upper contour must fulfill

$$H_u(r) > 0 \quad (18)$$

The maximum possible energy density with aluminium defined in Table II is

$$\kappa_{max} = \frac{X}{S \cdot \rho} = 14.15 \frac{Wh}{kg} \quad (19)$$

with a safety margin of 2.

The algorithm stopped at generation 69 and the result is shown in Fig. 3 and compared to the suggestion presented

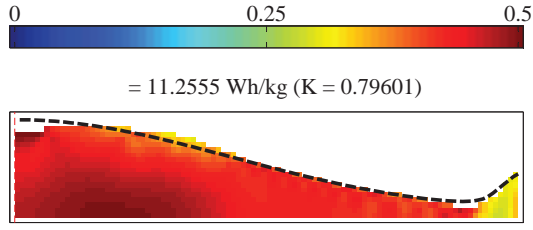


Figure 3. Optimization result with aluminium; Geometry factor $K = 0.80$; Suggestion of [3] for the CSD with $B = 5.25$, $\alpha_r = 4.89$, $h_c = 0.39$ and $\alpha_r = 0.0244$; Contour plot of von Mises yield criterion

in [3] with the parameters $B = 5.25$, $\alpha_r = 4.89$, $h_c = 0.39$ and $\alpha_r = 0.0244$. The results are in good agreement. On the axis of rotation the height is $H_u(r=0)/R_o = 0.18$ and then decreases to a minimum of $H_u(r/R_o=0.9)/R_o = 0.02$. At the outer radius a rim is formed with a height of $H_u(r=R_o)/R_o = 0.09$. The reached energy density is 11.26 Wh/kg , which corresponds to a geometry factor of $K = 0.80$.

B. Transverse Isotropic Material

Now also the lower rotor contour is unconstrained and optimized and the inner radius is no longer zero. The optimal rotor shape in the case of FRP is a thin cylinder with fibers in circumferential direction. Here the radial stress is very small and the whole load is carried by the fibers. For this reason an optimization algorithm will always try to converge to a thin cylinder. Therefore it will be requested that the rotor has a minimum radial thickness in the midplane

$$H_l(r \leq R_m) = 0 \quad (20)$$

with R_m as the minimal outer radius at $z = 0$. To achieve this the appropriate values of $\Delta h_{l,i}$ are removed from the vector of optimization variables, which yields to

$$\mathbf{x} = \left(h_{u,0}, \Delta h_{u,1}, \dots, \Delta h_{u,N-1}, \Delta h_{l,M}, \dots, \Delta h_{l,N-1} \right)^T \quad (21)$$

with

$$M = \left\lceil N \cdot \left(1 - \frac{R_m - R_i}{R_o - R_i} \right) \right\rceil \quad (22)$$

where $\lceil \dots \rceil$ is the ceil-operator.

Again 100 elements along the r -axis were used. Due to the manufacturing process the contour should increase monotonically, which is fulfilled by defining the optimization bounds as

$$\begin{aligned} 0 &\leq \Delta h_{u,i} \leq 4 \\ 0 &\leq \Delta h_{l,i} \leq 4 \end{aligned} \quad (23)$$

To achieve a reasonable rotor the following constraints were defined

$$\begin{aligned} \frac{R_i}{R_o} &= 0.3, & \frac{h_{u,0}}{h_{max}} &\geq 0.3, \\ \frac{R_m - R_i}{R_o - R_i} &\geq 0.3, & H_u(r) &> H_l(r) \end{aligned} \quad (24)$$

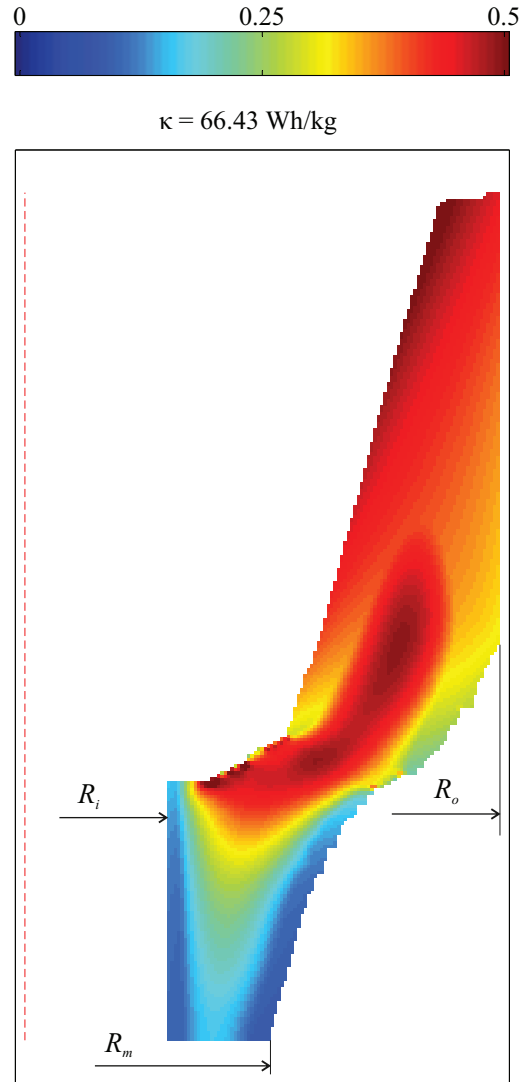


Figure 4. Optimization result after 83 generations with CFRP; $\kappa = 66.43 \text{ Wh/kg}$; Contour plot of Puck criterion

with

$$h_{max} = \frac{H_u(r = R_o)}{l_e} \quad (25)$$

The optimization result after 83 generations is shown in Fig. 4. An energy density of $\kappa = 66.43 \text{ Wh/kg}$ is reached. Due to the tendency to converge against a thin hollow cylinder, the constraints in (24) are active. The upper contour is flat starting from R_i , then a radius with a subsequent high slope is formed. Contrary H_l increases very fast and then flattens, therefrom in the shaft region, mass will be removed. In spite of decreasing moment of inertia the radial stress is reduced in this region enabling higher angular velocities. Here the highest specific stress is still in radial direction. The cantilever part is forming a hollow cone and the stresses are shifted in circumferential direction. Furthermore the slope of the upper contour leads to a larger radius of inertia and therefore an increase of performance.

Fig. 5 demonstrates the influence of the parameters listed

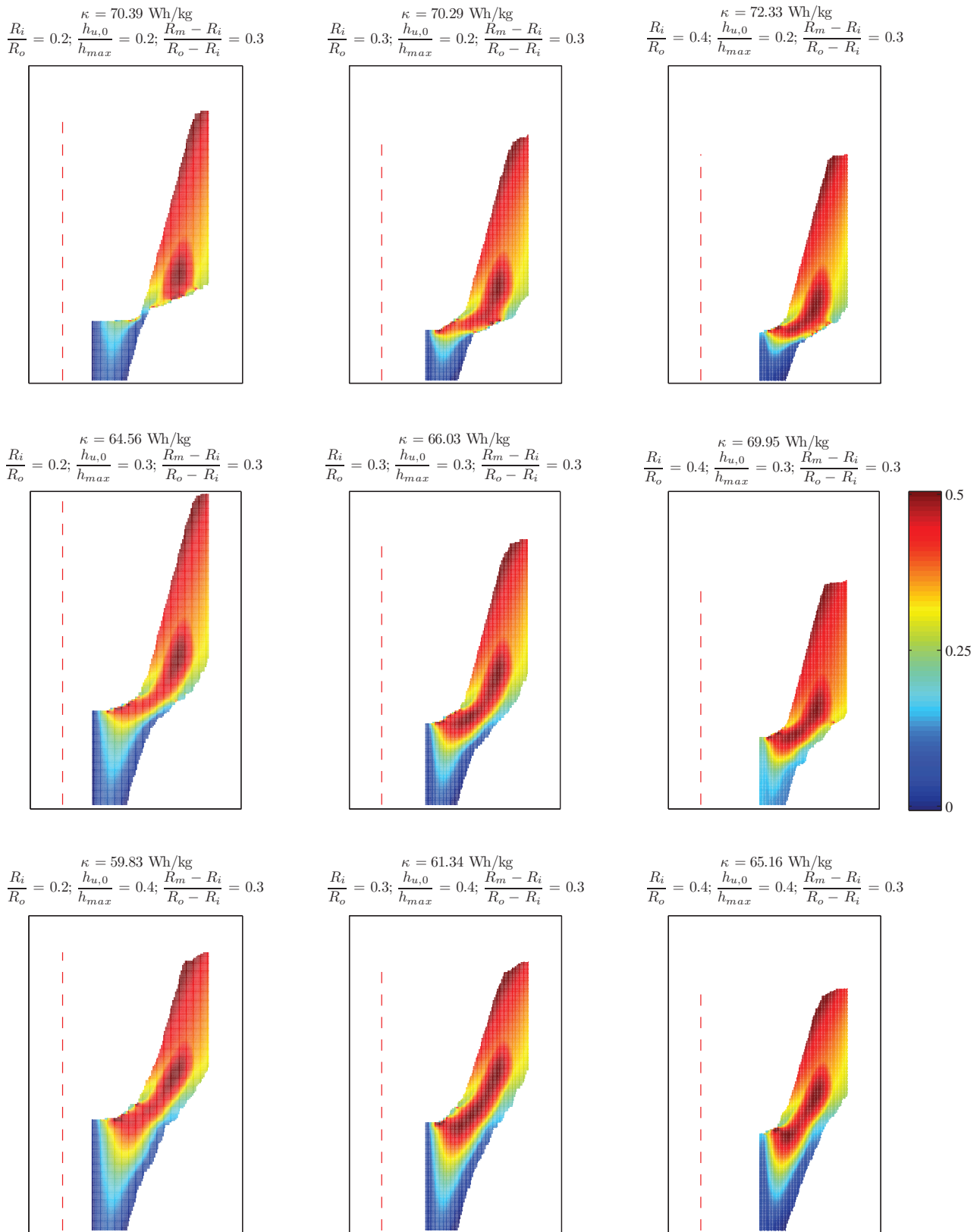


Figure 5. Optimization results for different sets of constraints; $(R_m - R_i)/(R_o - R_i) = 0.3$ and different values for R_i/R_o and $h_{u,0}/h_{max}$

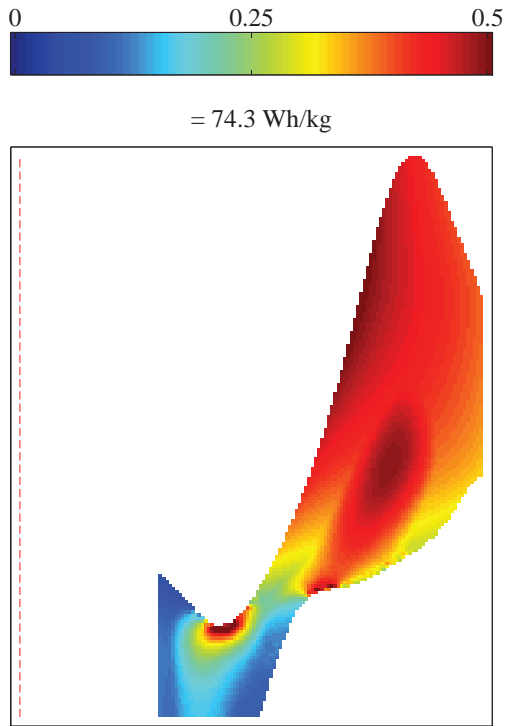


Figure 6. Optimization result after 84 generations with CFRP and non-monotonic rotor shape; $\kappa = 74.3 \text{ Wh/kg}$; Contour plot of Puck criterion

in (24). R_i/R_o and $h_{u,0}/h_{max}$ were varied with 0.2, 0.3 and 0.4 while $(R_m - R_i)/(R_o - R_i)$ was held constant at 0.3. The maximum value of the height h_{max} decreases with increasing R_i/R_o . In general the energy density increases with R_i/R_o . κ increases with decreasing values of $(R_m - R_i)/(R_o - R_i)$ and $h_{u,0}/h_{max}$. Low values of the height constraint are leading to a thin structure. The energy density can further be increased when the condition for monotonicity in (23) is dropped. In Fig. 6 the optimization result with

$$\begin{aligned} -4 \leq \Delta h_{u,i} \leq 4 \\ -4 \leq \Delta h_{l,i} \leq 4 \end{aligned} \quad (26)$$

as constraints, leading to a non-monotonic rotor shape, is shown. The upper contour was fitted to a polynomial of 12th order and the lower contour to one with 7th order to get a smoother rotor shape. One can see that the height at the beginning $h_{u,0}$ is rather low and the contour begins decreasing, forming a large radius to the cantilever. Furthermore the maximum height is smaller which leads to a more compact and plump structure. The lower contour is still monotonically increasing while the upper contour forms a tilted "S". Due to the larger radius at the beginning of the cantilever the energy density can be increased.

V. CONCLUSION

This paper presents the optimization of a FESS rotor by GA. A finite element model was used to find the shape of the CSD and furthermore a CFRP rotor was optimized for high performance FESS.

Improvements can be done by introducing triangular elements to get a smoother contour by avoiding sharp corners in the mesh. Also high numerical stresses can be avoided by advanced stress smoothing methods.

The optimized rotor shape can be manufactured just as a disc shaped rotor. The fibers are immersed in a resin bath and then wound on a mandrel. Care has to be taken in the area of the cantilever. When the inclination is too high, slipping of the fibers from the mandrel can occur. When the resin is cured, the mandrel can be removed. The whole rotor can be manufactured within one process or the outer contour can be filled and then formed by turning.

VI. ACKNOWLEDGMENT

The presented work is part of the research project "Optimum Shape-Flywheel" and is supported by "Klima und Energiefonds" in line with the program "NEUE ENERGIE 2020", conducted by the Austrian Research Promotion Agency (FFG).

REFERENCES

- [1] B. Bolund, H. Bernhoff, M. Leijon M, "Flywheel energy and power storage systems," *Renewable and Sustainable Energy Reviews* 11 (2007) 235-258.
- [2] G. Genta, "Kinetic energy storage, theory and practice of advanced flywheel systems", *Butterworths*, London Boston, 1985.
- [3] G. Genta, "Some considerations on the constant stress disc profile", *Meccanica*, December 1989, Vol. 24, Issue 4, pp. 235-248.
- [4] S.K. Ha, D.J. Kim and T.H. Sung, "Optimum design of multi-ring composite flywheel rotor using a modified generalized plane strain assumption", *International Journal of Mechanical Sciences*, 43 (2001) 993-1007.
- [5] J.D. Kwon, S.J. Kim, S.U. Nasir, S.K. Ha, "Design and Fabrication of Hybrid Composite Flywheel Rotor," *World Academy of Science, Engineering and Technology* 60, 2011.
- [6] R. Okou, A.B. Sebitosi, A. Pillay, "Flywheel rotor manufacture for rural energy storage in sub-Saharan Africa", *Energy*, Vol. 36, Issue 10, Oct. 2011, pp. 6138-6145.
- [7] M.P. Bendsøe, O. Sigmund, "Topology Optimization, Theory, Methods and Applications", Springer-Verlag Berlin Heidelberg, 2003.
- [8] J.S. Liu, G.T. Parks, P.J. Clarkson, "Optimization of Turbine Disk Profiles by Metamorphic Development", *Journal of Mechanical Design*, 2002.
- [9] D. Eby, R.C. Averill, W.F. Punch, E.D. Goodman, "Optimal design of Flywheels using an injection island genetic algorithm," *Artificial Intelligence for Engineering Design, Analysis and Manufacturing - AI EDAM*, Vol. 13, pp. 327-340.
- [10] D. Hockney, D. Ansbegian, M. Polimeno, W. Spears, A. Palazzolo, S. Pekarek, "Extreme Energy Density Flywheel Energy Storage System for Space Applications", *6th International Energy Conversion Engineering Conference (IECEC)*, Ohio, Juli 2008.
- [11] A. Puck, H. Schürmann, "Failure analysis of FRP laminates by means of physically based phenomenological models", *Composites Science and Technology* 62 (2002) 1633-1662.
- [12] A. Puck, J. Kopp, M. Knops, "Guidelines for the determination of the parameters in Puck's action plane strength criterion", *Composites Science and Technology* 62 (2002) 371-378.
- [13] M.J. Hinton, A.S. Kaddour, P.D. Soden, "A comparison of the predictive capabilities of current failure theories for composite laminates, judged against experimental evidence," *Composites Science and Technology* 62 (2002) 1725-1797.